International Journal of Electrical, Electronic and Communication Sciences
ISSN: 2517-9438
Vol:9, No:2, 2015

Effects of Position and Shape of Atomic Defects on the Band Gap of Graphene Nano Ribbon Superlattices

Zeinab Jokar, Mohammad Reza Moslemi

***Abstract*—**In this work, we study the behavior of introducing atomic size vacancy in a graphene nanoribbon superlattice. Our investigations are based on the density functional theory (DFT) with the Local Density Approximation in Atomistix Toolkit (ATK). We show that, in addition to its shape, the position of vacancy has a major impact on the electrical properties of a graphene nanoribbon superlattice. We show that the band gap of an armchair graphene nanoribbon may be tuned by introducing an appropriate periodic pattern of vacancies. The band gap changes in a zig-zag manner similar to the variation of band gap of a graphene nanoribbon by changing its width.

***Keywords*—**Antidot, Atomistix ToolKit, Superlattice, Vacancy.

I. Introduction

GRAPHENE is a single atomic layer consisting of a two-dimensional honeycomb lattice of carbon atoms that invented by [1]. This novel system has attracted intense attention because of new fundamental physics and promising applications in nanoelectronics. It exhibits high crystal quality and ballistic transport properties on a submicron scale. Graphene samples are usually fabricated by micromechnical cleavage of graphite and have excellent mechanical properties that make it possible to sustain huge electric currents [2]-[4]. One of the other interesting properties of graphene is its Dirac-type spectrum [5]. On the other hand, the confinement of Dirac fermions at a nanometer scale is one of the central goals of graphene-based electronics and has attracted increasing interest. In recent years, it was demonstrated experimentally that graphene can be cut in the desired shape and size [6], [7]. Recent progresses in fabricating and characterizing stable graphene nanostructures provides the opportunity to explore the various remarkable optical and transport properties of these structures [8]-[11]. For this reason, the change in the bandgap of graphene likes an artificial origami. The Graphene Nano Ribbons (GNRs) of width less than 10 nm exhibit a large bandgap which makes them suitable for electronic devices [7]. Because of the difficulties in fabricating sub-10 nm nanoribbons and also the importance of the edge effects in such GNRs, researchers have devised new means to modulate the electronic band structure of GNRs in order to make them suitable for different electronic and optical applications. These methods include applying disorder [12], doping [13], external fields [14], or mechanical strain [15]-[19]. However, because of the difficulties of applying strain, Recently, both experimental and theoretical works have addressed the possibility to create on graphene, a single or a few number of vacancies, or even a superlattice of vacancies [20]-[23]. The formation of vacancy defects in infinite graphene has been studied using a number of computational methods [24], [25]. The electronic properties of hydrogenated graphene superlattice with a single vacancy (antidot) in the unit cell have been also discussed in the literature [21]. They studied the dependence of the electronic and transport properties of AGNR antidot superlattices on the details of the geometrical configuration of the systems. The transport behavior of these complex systems is defined by the new electronic energy states and forbidden energy regions which appear due to the extra electronic confinement potential and the new types of symmetries imposed by the periodic vacancies in the lattice. However, the vacancies are considered in the center of unit cell.

Here, we study the electronic band structure of some extra types of graphene antidot superlattices compared to [21] by changing the position of vacancies among the width of unit cell. Our simulations are based on density functional theory (DFT) with an ab-initio along with the local density approximation (LDA). In this paper we use Atomistix Toolkit (ATK) package. The paper is organized as follows. In Section II we introduce the proposed structure and the simulation method. In Section III, we will conclude the paper.

II. Modeling and Simulations

Fig. 1 illustrates different configurations of defects in the unit cell of an N = 11 AGNR considered in this study. The desired superlattice structure could be formed by periodic repeat of this unit cell. The types of defects showed in this figures are as follow: (a) linear-type defect with two atoms extracted, (b) diagonal-type defect with two atoms extracted, (c) triangle-type defect with four vacancy sites, (d) hexagon-type defect with six extracted atoms, (e) symmetric rhomboid-type defect and (f) asymmetrical rhomboid-type defect with eight extracted atoms. Here, d is the width of the unit cell and represents the distance between two adjacent defects in the superlattice.

Zeinab Jokar is with the Department of electrical and electronics, Sepidan Branch, Islamic Azad University, Sepidan, Iran.

Mohammad Reza Moslemi is with the Department of electrical and electronics, Zarghan Branch, Islamic Azad University, Zarghan, Iran (corresponding author to provide e-mail: moslemi@zariau.ac.ir).

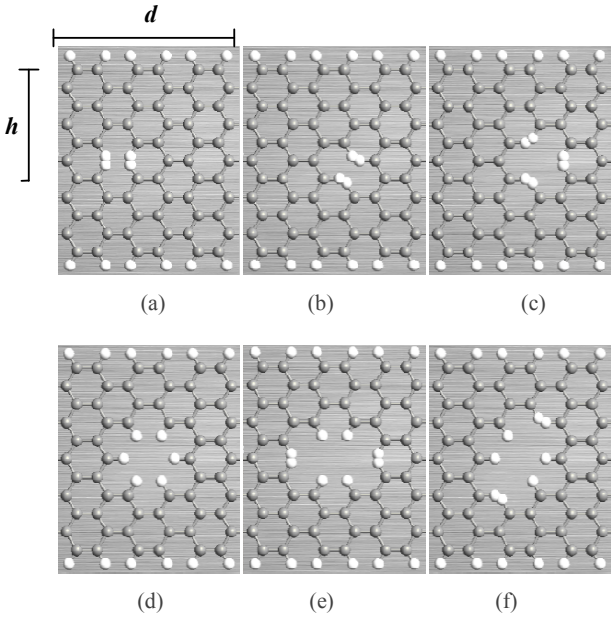

Fig. 1 The schematic view of unit cells of six different superlattices with (a) linear (b) diagonal (c) triangle (d) hexagon (e) symmetric rhomboid (f) asymmetrical rhomboid defects

Also, h indicates the latitude of the first extracted atom compared to the top of unit cell. The band structure and density of states (DOS) of these superlattices compared by changing the parameters defined earlier. The simulations are based on density functional theory (DFT) with an ab-initio along with the local density approximation (LDA) and taking into account an energy cutoff equal to 150 Ry. In this paper we use Atomistix Toolkit (ATK) package. The transport properties of the system are calculated using Non-equilibrium Green's Function (NEGF) in the real space mode. Using the Green's function method, the transmission function may be written as:

$$T(E) = Tr\left(\Gamma_L G_C^{ret} \Gamma_R G_C^{adv}\right) \quad (1)$$

where $G_C^{ret/adv}(E)$ is the retarded and advanced Green's function and $\Gamma_{L/R}(E)$ is the coupling between the central part and two semi-infinite ribbons. The conductance is then calculated using the Landauer formalism.

$$G(E) = \frac{2e^2}{h} T(E) = \frac{2e^2}{h} Tr\left(\Gamma_L G_C^{ret} \Gamma_R G_C^{adv}\right) \quad (2)$$

The band structure of perfect N = 11 AGNR calculated based on the above theorem and plotted in Fig. 2. As shown in this figure, this nanoribbon is a semiconductor with a band gap about 0.2 eV. This is due to the fact that the N = 3q+2 and the third nearest neighbor atoms interactions form a small bandgap.

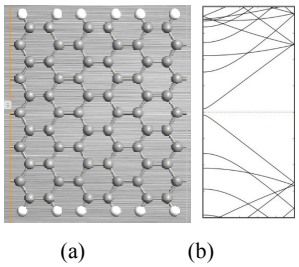

Fig. 2 (a) Unit cell of the considered perfect N = 11 AGNR and (b) Its electronic band structure

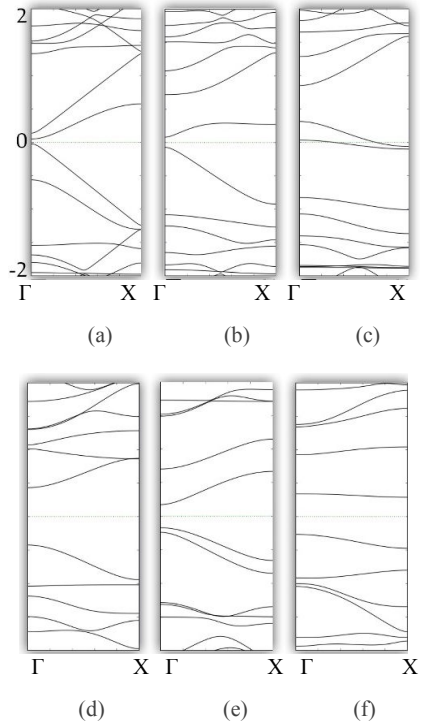

Fig. 3 Band structures of superlattices with (a) linear-type (b) diagonal-type (c) triangle-type (d) hexagon-type (e) symmetric rhomboid-type (f) asymmetrical rhomboid-type defects for h = 6.

The band structures of six superlattices shown in Fig. 1 are plotted in Fig. 3 assuming that the lattice defects are located in the center of the unit cell with d = 3 and h = 6. Here, we extract 2, 4 and 6 carbon atoms in different shapes from the unit cell. As shown in this figure, the band structure is strongly influenced by vacancies. For example, when we apply a triangle-type defect the conduction and valence bands penetrates into together and the nanoribbon shows fully metallic behavior, as shown in Fig. 3 (c). Also, the GNR would have an indirect bandgap when an asymmetrical rhomboid defect applied to the center of unit cell. Further, the bandgap is about 0.02 eV in Fig. 3 (a) which is smaller than that of the perfect 11-AGNR. The hexagon-type vacancy causes the largest bandgap which is about 0.86 eV. Next, we change the position of vacancy in the zigzag direction of AGNR by changing h. Due to the symmetrical properties, we only increase h. Fig. 4 shows the band structures

corresponding to vacancies as shown in Fig. 1 but for h = 7. As shown in this figure, the change in the position of vacancies could result a meaningful variations in band structures like increasing bandgap in Figs. 4 (a) and (e). Fig. 4 (f) shows that the GNR behaves as a metal for h = 7.

The band structures of eight different vacancies for h = 8 and h = 9 are shown in Figs. 5 and 6. The band structures have also changed in these figures compared to previous types and positions of vacancies. Comparison of Figs. 2 to 6 reveals that the energy gap will change when the shape of vacancy changes. Our simulations show that in addition of the shape, the location of vacancies have also a big influence on the band gap.

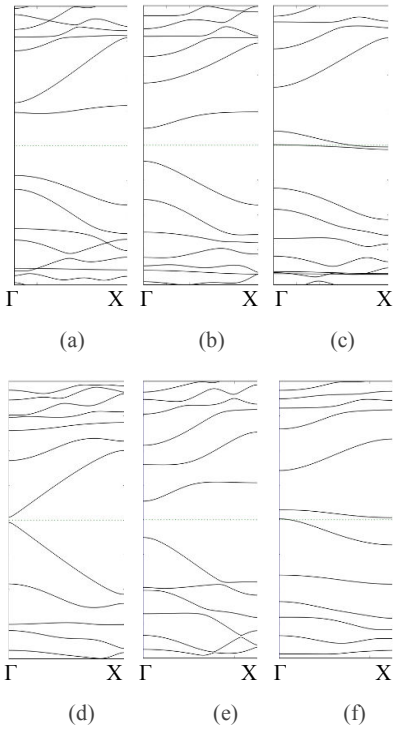

Fig. 4 Band structures of superlattices with (a) linear-type (b) diagonal-type (c) triangle-type (d) hexagon-type (e) symmetric rhomboid-type (f) asymmetrical rhomboid-type defects for h = 7

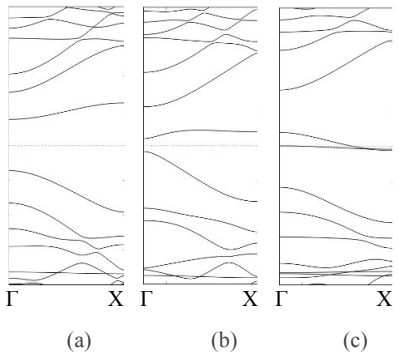

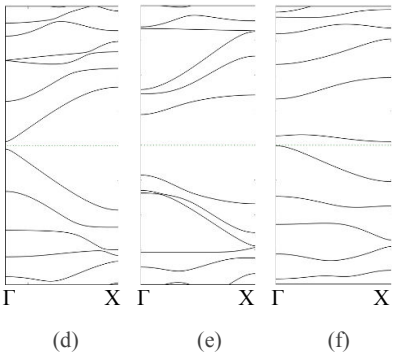

Fig. 5 Band structures of superlattices with (a) linear-type (b) diagonal-type (c) triangle-type (d) hexagon-type (e) symmetric rhomboid-type (f) asymmetrical rhomboid-type defects for h = 8.

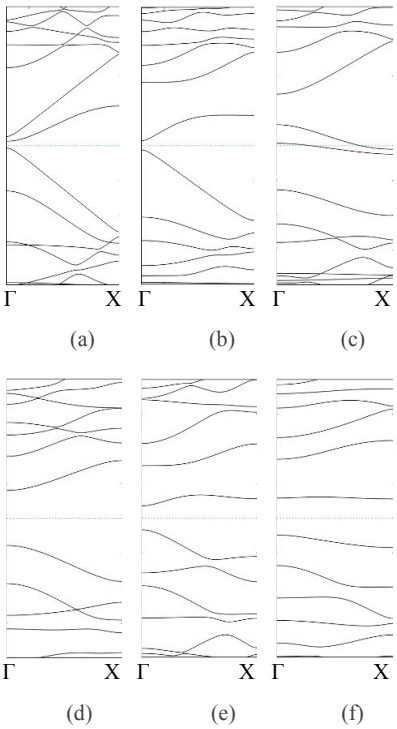

Fig. 6 Band structures of superlattices with (a) linear-type (b) diagonal-type (c) triangle-type (d) hexagon-type (e) symmetric rhomboid-type (f) asymmetrical rhomboid-type defects for h = 9

TABLE I
LIST OF BAND GAPS FOR DIFFERENT TYPES AND LOCATIONS OF VACANCIES SHOWED IN FIG. 3-6.

VACANCY	A	B	C	D	E	F
$H=6$	0.09	0.13	metallic	0.86	0.34	0.56
$H=7$	0.9	0.48	metallic	0.09	0.52	metallic
$H=8$	0.73	0.19	metallic	0.12	0.87	0.07
$H=9$	0.89	0.14	metallic	0.79	0.34	0.52

The band gaps related to different vacancies are listed in Table I. In order to better comparison, we plot the variations of band gaps for all different types of vacancies versus their locations in Fig. 7. Simulation results show that the maximum band gap relates to linear-type vacancy with h = 7. Also, regardless of its location, the triangle-type vacancy causes the metallic properties of graphene nanoribbon. This behavior is due to the zig-zag edges of graphene nanoribbons at both sides of vacancy. In other words, the vacancy converts the 12-AGNR to two nanoribbons with new width and number of dimmer atoms (N). In the case in which the vacancy is triangle-type, both of two new ribbons are zig-zag and show metallic behavior. In other cases, the band gap shows a reciprocating behavior as plotted in Fig. 7. The band gap changes of Fig. 7 are similar to the band gap variation versus width of an armchair graphene nanoribbon. In fact, the width of new ribbons around the vacancy may change by varying the location of vacancy.

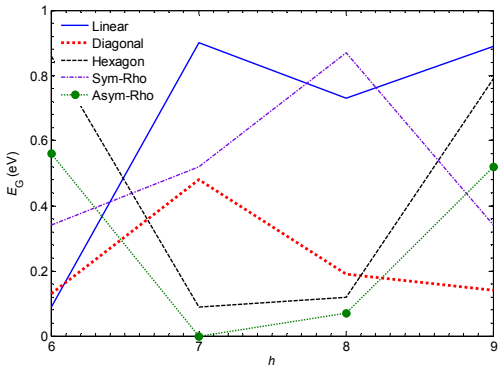

Fig. 7 Variations of band gaps for different types of vacancies versus their locations (h)

III. CONCLUSION

In this paper, the density functional theory (DFT) with an ab-initio along with the Local Density Approximation is used in Atomistix Toolkit package to analyze the effects of shapes and position of atomic size defects on the band structure of GNR superlattices. Six different types of atomic size vacancy is applied to a superlattice of 11-AGNR with d = 3. Simulations show meaningful changes on the band structure of the GNR. The band gap of the graphene nanoribbon could be tuned by changing the periodic pattern of the vacancy instead of changing its width. Some vacancies cause the GNR superlattice to show metallic behavior regardless of their positions. Then the vacancies lowered across the width of superlattice's unit cell. The simulations showed zig-zag variations in the band gap of GNR by changing the position of vacancy across the width. The maximum band gap relates to a linear-type vacancy with h = 7.

ACKNOWLEDGMENT

We gratefully acknowledge the support and corporation of Sepidan and Zarghan Branches of Islamic Azad University, without which the present study could not have been completed. The research for this paper was accomplished in Sepidan Branch, IAU as M.Sc. thesis.

REFERENCES

[1] K.S. Novoselov, A.K. Geim, S.V. Morozov, D. Jiang, Y. Zhang, S.V. Dubonos, I.V. Grigorieva, A.A. Firsov, "Electric Field Effect in Atomically Thin Carbon Films," in Science, 306, 2004, pp. 666-669.
[2] P. G. Silvestrov and K. B. Efetov, "Quantum dots in graphene," in Phys. Rev. Lett. 98, 2007, pp. 016802.
[3] A. DeMartino, L. Dell'Anna, and R. Egger, "Magnetic Confinement of Massless Dirac Fermions in Graphene," in Phys. Rev. Lett. 98, 2007, pp. 066802.
[4] H. Y. Chen, V. Apalkov, and T. Chakraborty, "Fock-Darwin States of Dirac Electrons in Graphene-Based Artificial Atoms," in Phys. Rev. Lett. 98, 2007, pp. 186803.
[5] M. I. Katsnelson, K. S. Novoselov, A. K. Geim, "Klein Tunneling in Graphene," in Nature Physics 2, 2006, pp. 620 – 625.
[6] D. Unluer, F. Tseng, A. Ghosh, M. Stan, "Monolithically patterned wide-narrow-wide all-graphene devices," in Nanotechnology, IEEE Transactions on, 10, 2011, pp. 931- 939.
[7] X. Wang, Y. Ouyang, X. Li, H. Wang, J. Guo, H. Dai, "Room-Temperature All-Semiconducting Sub-10-nm Graphene Nanoribbon Field-Effect Transistors," in Physical Review Letters, 100, 2008, pp. 206803.
[8] Jingwei Bai, Yu Huang, "Fabrication and electrical properties of graphene nanoribbons," in Materials Science and Engineering R 70, 2010, pp. 341–353.
[9] Yun-Sok Shin, Jong Yeog Son, Moon-Ho Jo, Young-Han Shin, Hyun Myung Jang, "High-Mobility Graphene Nanoribbons Prepared Using Polystyrene Dip-Pen Nanolithography," in J. Am. Chem. Soc., 133, 2011, pp. 5623–5625.
[10] Timothy H. Vo, Mikhail Shekhirev, Donna A. Kunkel, Martha D. Morton, Eric Berglund, Lingmei Kong, Peter M. Wilson, Peter A. Dowben, Axel Enders, Alexander Sinitskii, "Large-scale solution synthesis of narrow graphene nanoribbons," in Nature Communications, 5, 2014, pp. 3189.
[11] Kyung Tae Kim, Jae Woong Jung, Won Ho Jo, "Synthesis of graphene nanoribbons with various widths and its application to thin-film transistor," in Carbon, 63, 2013, pp. 202–209.
[12] B. Biel, X. Blase, F. Triozon, S. Roche, "Anomalous Doping Effects on Charge Transport in Graphene Nanoribbons," in Physical Review Letters, 102, 2009, pp. 096803.
[13] B. Huang, Q. Yan, G. Zhou, J. Wu, B.L. Gu, W. Duan, F. Liu, "Making a field effect transistor on a single graphene nanoribbon by selective doping," in Applied Physics Letters, 91, 2007, pp. 253122.
[14] Y.W. Son, M.L. Cohen, S.G. Louie, "Half-metallic graphene nanoribbons," in Nature, 444, 2006, pp. 347-349.
[15] N. Ferralis, R. Maboudian, C. Carraro, "Evidence of structural strain in epitaxial graphene layers on 6H-SiC (0001)," in Physical Review Letters, 101, 2008, pp. 156801.
[16] M. Teague, A. Lai, J. Velasco, C. Hughes, A. Beyer, M. Bockrath, C. Lau, N.C. Yeh, "Evidence for strain-induced local conductance

modulations in single-layer graphene on SiO2," Nano letters, 9, 2009, pp. 2542-2546.
[17] M. Topsakal, S. Cahangirov, S. Ciraci, "The response of mechanical and electronic properties of graphane to the elastic strain," in Applied Physics Letters, 96, 2010, 091912.
[18] Y. Gao, P. Hao, "Mechanical properties of monolayer graphene under tensile and compressive loading," Physica E: Low-dimensional Systems and Nanostructures, 41, 2009, pp. 1561-1566.
[19] M.R. Moslemi, M.H. Sheikhi, K. Saghafi, M.K. Moravej-Farshi, "Electronic properties of a dual-gated GNR-FET under uniaxial tensile strain," in Microelectronics Reliability, 52, 2012, pp. 2579.
[20] T. G. Pedersen, C. Flindt, J. Pedersen, N. A. Mortensen, A.-P. Jauho, and K. Pedersen, "Graphene Antidot Lattices: Designed Defects and Spin Qubits," in Phys. Rev. Lett. 100, 2008, pp. 136804.
[21] L. Rosales, M. Pacheco, Z. Barticevic, A. León, A. Latge, P. A. Orellana, "Transport properties of antidot superlattices of graphene nanoribbons," in Phys. Rev. B. 80, 2009, pp. 073402.
[22] Jing-Jing Chen, Han-Chun Wu, Da-Peng Yuab, Zhi-Min Liao, "Magnetic moments in graphene with vacancies," in Nanoscale, 15, 2014.
[23] Yamada Y, Murota K, Fujita R, Kim J, Watanabe A, Nakamura M, Sato S, Hata K, Ercius P, Ciston J, Song CY, Kim K, Regan W, Gannett W, Zettl A, "Subnanometer vacancy defects introduced on graphene by oxygen," in J. Am. Chem. Soc., 2014, pp. 2232-5.
[24] G.D. Lee, C.Z. Wang, E. Yoon, N.M. Hwang, D.Y. Kim, K.M. Ho, "Diffusion, Coalescence, and Reconstruction of Vacancy Defects in Graphene Layer," in Phys. Rev. Lett. 95, 2005, pp. 205501.
[25] H. Zhang, M. Zhao, X. Yang, H. Xia, X. Liu, Y. Xia, "Diffusion and coalescence of vacancies and interstitials in graphite: A first-principles study," in Diamond and Related Materials, 19, 2010, pp. 1240-1244.

Mohammad Reza Moslemi was born in Nowshahr, Islamic Republic of IRAN, on May 10, 1976. He graduated in B.Sc. from the Sharif University of technology. His M.Sc. was in Shiraz school of engineering in electronics. He graduated in Ph.D. from Research and Science Branch, IAU in 2013.

His special field of interest included nano electronic and nano devices based on carbon based materials. He is a member of iranian national national elite foundation.